Preprints (www.preprints.org) | NOT PEER-REVIEWED | Posted: 27 October 2018 doi:10.20944/preprints201810.0643.v1

Peer-reviewed version available at *Water* **2019**, *11*, 78; doi:10.3390/w11010078

Assimilation of Synthetic SWOT River Depths in a Regional Hydrometeorological Model

Vincent Häfliger[1, 2], Eric Martin[1,3], Aaron Boone[1], Sophie Ricci[4], Sylvain Biancamaria[5]

[1]CNRM-GAME, UMR 3589, Météo-France, CNRS, Toulouse, France

[2]Meteorologisches Institut, Bonn Universität, Bonn, Germany

[3]IRSTEA, UR RECOVER, Aix-en-Provence, France

[4]CECI, CERFACS-CNRS, 42 avenue G. Coriolis, 31057 Toulouse, France

[5]CNRS, LEGOS, UMR 5566-CNRS-CNES-IRD-Université Toulouse III, Toulouse, France

Correspondence to: Vincent Häfliger (vincent.haefliger@yahoo.fr)

Key words: overland flow, satellite altimetry, hydrological modelling, data assimilation

Abstract. The Surface Water and Ocean Topography (SWOT) mission, to be launched in 2021, will provide water surface elevations, slopes, and river width measurements for rivers wider than 100 m. In this study, synthetic SWOT data are assimilated in a regional hydrometeorological model in order to improve the dynamics of continental waters over the Garonne catchment, one of the major French catchments. The aim of this paper is to demonstrate that the sequential assimilation of SWOT-like river depths allows the correction of river bed roughness coefficients and thus simulated river depths. An extended Kalman Filter is implemented and the data assimilation strategy was applied to four experiments of gradually increasing complexity regarding observation and model error over the 1995-2000 period. With respect to a "true" river state, assimilating river depths allows the proper retrieval of constant and spatially distributed roughness coefficients with a root mean square error of 1 $m^{1/3} s^{-1}$, and the estimation of associated river depths. It was also shown that river depth differences can be assimilated, resulting in a higher root mean square error for roughness coefficients with respect to the true river state. The last study shows how one can take into account more realistic sources of SWOT error measurements, in particular the importance of the estimation of the tropospheric water content in the process.

© 2018 by the author(s). Distributed under a Creative Commons CC BY license.

Preprints (www.preprints.org) | NOT PEER-REVIEWED | Posted: 27 October 2018 doi:10.20944/preprints201810.0643.v1

Peer-reviewed version available at Water 2019, 11, 78; doi:10.3390/w11010078

1. Introduction

Surface water storage and fluxes in rivers, lakes, reservoirs and wetlands are currently poorly observed at a regional scale, even though they represent major components of the water cycle and impact deeply human societies (Biancamaria et al. 2016), both in terms of water resources and catastrophe events such as floods. In situ networks are heterogeneously distributed in space, and many river basins and most lakes – especially in the developing world and in sparsely populated regions – remain unmonitored (Biancamaria et al. 2010). The continental water cycle can be formulated in a simple mass balance equation, linking the total water storage variation in time (ΔS) with different water fluxes between the continental surface, the atmosphere, and the underground domain: these are precipitations (P), evapotranspiration (E), the infiltration in the subsurface (I), and the overland flow (Q). The mass balance equation simply assumes that the total water storage variation ΔS is equal to the precipitations P from which are subtracted the terms E, Q, and I. Altimetry products from remote sensing are increasingly used for the monitoring of these hydrological cycle components. Several altimetric satellites have been launched in the past to measure water surface elevations, among which ERS-1 (1991-2000), TOPEX/Poseidon (1992-2006), ERS-2 (1995-2003), Jason-1 (2001-2013), Envisat (2002-2012), Jason-2 (2008-now), and SARAL (2013-now). They provide repetitive water elevation measurements on a global scale, something which is particularly important for ungauged basins. They do however have many limitations, such as their long revisit time (between 10 and 35 days; Santos da Silva et al. 2010), and their coarse spatial resolution; instruments' footprints are several square km and they only observe from their nadir (from the vertical of the satellite). In order to overcome these limitations, Alsdorf et al. (2007) proposed a new satellite mission based on synthetic aperture radar (SAR) interferometry. This was called Water and Terrestrial Elevation Recovery (WATER), providing water elevation maps for two 50 km swaths. In 2007, the National Research Council recommended this new satellite mission to NASA, under the name Surface and Ocean Topography (SWOT), so as to measure both the ocean and land water surface topography. This new mission, conjointly developed by NASA, CNES (Centre National d'Etudes Spatiales), CSA/ASC (Canadian Space Agency/Agence Spatiale Canadienne) and UKSA (United-Kindom Space Agency), is planned for launch in 2021 and will observe the whole continental water-estuaries-ocean continuum. SWOT is designed to observe a large fraction of rivers and lakes globally and will provide observations of their seasonal cycles. SWOT will be the first altimetry mission to observe intermediate (or regional)-scale basins with a relatively high frequency, i.d. for temperate regions such as western Europe: 50 000 – 200 000 km^2, providing a quasi-global coverage of between 78°S and 78°N in 21 days, the duration of a full orbital cycle (Pavelsky et al. 2014). Water level measurement errors are expected to be 10cm aggregating pixels over a 1 km^2 water area (e.g., a 10-km reach length for a 100-m-wide river) (Rodríguez 2016). This offers a new opportunity for the linking of open water surface elevations, land surface processes, and meteorology more closely on this scale. Thanks to the SWOT mission, the evolution in terms of the time of the surface water storage will be revealed. This information will allow a better understanding of the term Q both spatially and temporally playing an important role in the mass balance equation.

Data assimilation (DA) techniques are increasingly used by hydrologists to improve the performance of numerical models. The DA techniques are used to correct either the model parameters and/or the model state. The merits of remotely sensed DA have been shown in various studies. Zaitchik et al. (2008) used GRACE data on total water storage over the Mississipi river, in order to improve the soil water content and different water fluxes in the basin. In the field of wide swath altimetry, Biancamaria et al. (2011) assimilated synthetic SWOT data in the Arctic Ob River in Siberia, in order to improve water elevation and discharge: the combination of hydrologic and hydraulic models with the SWOT data allows to better describe temporal variations of open water surface elevations. At large scale catchment, Pedinotti et al. (2014) assimilated synthetic SWOT data in the Niger basin to correct the roughness coefficient of the river bed, in order to better represent river discharge and flood plain dynamics. These examples demonstrate the strong capability of spa-

Preprints (www.preprints.org) | NOT PEER-REVIEWED | Posted: 27 October 2018 doi:10.20944/preprints201810.0643.v1

Peer-reviewed version available at Water 2019, 11, 78; doi:10.3390/w11010078

tialized satellite information to improve our knowledge of the continental hydrological cycle. Wide swath altimetry measurements made by the SWOT satellite mission will provide the potential for high-resolution characterization of open water surface elevations and will contribute to a fundamental understanding of the global water cycle by providing global measurements of terrestrial surface water storage changes and discharge.

Most of these DA studies focus on big river basins. This paper aims to focus on a regional scale, what is something new according to the author's knowledge. The time evolution of physical processes is faster, and it is important to analyze whether or not the information given by SWOT will be able to improve our understanding of the hydrological cycle on this spatial and temporal scale. Häfliger et al. (2015) assessed the ability of a regional hydrometeorological model to simulate river depths comparable with the future SWOT open surface water elevation observations. The river depth is equal to the vertical distance between the river bed and the open surface water elevation of the river. The distributed ISBA/MODCOU (Interaction Soil Biosphere Atmosphere / MODèle COUplé) model was used over the Garonne catchment, taking into account a variable flow velocity in the river channel. This kinematic wave formulation is used in the present study in the form of the Manning-Strickler equations, derived from the full Saint-Venant equation system. It takes into consideration that there is no diffusion of the flood wave from upstream to downstream in the river. In the present study, synthetic SWOT-like data are assimilated into a regional scale hydrological model over the Garonne catchment in the South-West of France. The study is based on the previous numerical developments for the implementation of data assimilation achieved by Pedinotti et al. (2014) but is focused on a smaller basin located in another climatic region and uses a different hydrological model.

This work is carried out in the framework of Observing System Simulation Experiment (OSSE) with the ISBA/MODCOU hydrometeorological model to prepare future exploitation of the SWOT data. The paper is divided into five sections. Section 2 presents the Garonne catchment and the ISBA/MODCOU model that simulated river depths. The DA strategy is developed in Section 3: a short description of the SWOT mission is given, the OSSE framework is explained and the filtering data assimilation algorithm is presented along with its implementation. Results are presented in Section 4 on four different experimental settings. Conclusions and perspectives concerning DA strategy and link with the SWOT mission are finally given in Section 5.

2. Catchment and hydrological model description

2.1. The Garonne river catchment

The study is carried out over the Garonne River catchment (Fig. 1). The Garonne catchment is one of the major catchments in France (56 000 km²) with a river width ranging from 150 m in Toulouse to 300 m near Bordeaux. It is located in southwestern France and drains the northern slopes of the Pyrenees chain (along the French border with Spain). The Pyrenees and the Massif Central mountains border the basin to the south and the east, respectively. The main tributaries of the Garonne river are the Tarn and Lot rivers. The climate over the basin is under the influence of oceanic conditions over the western part of the domain characterized by heavy rainfall events during winter and relatively warm weather during summer. There is a significant precipitation gradient from West to East, ranging from approximately 1’200 mm year $^{-1}$ over the Atlantic coastal region to about 600 mm year $^{-1}$ 300 km to the East. The upper Garonne and the Ariège rivers regime is characterized by spring snow melt in the Pyrenees (Caballero et al., 2007), while summer flows are very low due to relatively dry summers.

2.2 The ISBA/MODCOU hydrological model

The ISBA land surface model (Noilhan and Planton 1989) within the Surface Externalisée (SURFEX) platform (Masson et al. 2013) is used to simulate the physical variables every 3 hours in the upper soil, soil surface, and vegetation and to simulate water and energy exchanges within the soil–surface–atmosphere continuum. Its parameters are derived

Preprints (www.preprints.org) | NOT PEER-REVIEWED | Posted: 27 October 2018 doi:10.20944/preprints201810.0643.v1

Peer-reviewed version available at Water 2019, 11, 78; doi:10.3390/w11010078

from the ECOCLIMAP2 ecosystems and surface parameters database (Faroux et al. 2013) at a 1-km resolution. ISBA is forced every 3 hours by the SAFRAN meteorological analysis (Durand et al. 1993). ISBA uses a multilayer approach to solve the one-dimensional Fourier law and the mixed form of the Richards equation explicitly in order to calculate the time evolution of the soil energy and water budgets (Boone et al. 2000; Decharme et al. 2011). In terms of hydrology, the soil water balance accounts for infiltration, land surface evapotranspiration, and total runoff. The infiltration rate is provided by the difference between the through fall rate and the surface runoff. The throughfall rate is the sum of the rainfall not intercepted by the canopy, the dripping from the interception reservoir, and the snowmelt from the snow-pack (Decharme et al. 2013). The total runoff is composed of the surface runoff, a lateral subsurface flow in the topsoil, and a free drainage condition at the bottom of the hydrological soil column.

The hydrological and hydrogeological model platform MODCOU routes the continental surface water into the river. The surface runoff simulated by ISBA is transferred to the river by the isochrone transfer (ISO) module (Ledoux et al. 1984). Water is then routed within the river by the parallel-computing-based RAPID module (David et al. 2011a, b), with a spatial resolution of 1 or 2 km. MODCOU is the name given to the full platform with its two components ISO and RAPID. The kinematic wave method is used for the river transfer routing RAPID, with the implementation of the Manning-Strickler equations. The equation linking the river depth and the roughness coefficient is the following (Eq. 1):

$$h(K_{str}) = \left(\frac{Q}{K_{str} \cdot W \cdot \sqrt{S_o}}\right)^{\frac{3}{5}} \quad (1)$$

where h is the river depth [m], K_{str} is the Strickler coefficient [$m^{1/3}$ s^{-1}], Q is the discharge [m^3 s^{-1}], W is the width [m], and S_o is the bed slope [-]. The formulation is derived from the full Saint-Venant equation system, and supposes that the bed slope S_o of the river bed is entirely compensated by the friction slope S_f. Thus $S_o = S_f$ means that there is no diffusion but a simple translation in the time of the flood wave along the river channel. The K_{str} coefficients are supposed to be constant over time and are spatially distributed for each grid cell of the model. The bed slopes S_o are calculated from The Digital Elevation Model SRTM 90 m (Farr et al. 2007) in the full river network of the Garonne catchment. The discharge regime is permanent and uniform in each grid cell of the model, where the values of the water storage, the discharge and the river depth simulation are solved with a «Runge-Kutta order 4» method to prevent numerical bias caused by the nonlinearity of the Manning-Strickler formula (Decharme et al. 2010). This routing method is used in global hydrological models (e.g. in the TRIP model: Decharme et al. 2010, Alkama et al. 2010, Pedinotti et al. 2012) or in the regional ISBA/MODCOU model (Häfliger et al. 2015). In the present paper, a time step of 300 s is chosen for the river routing, and the geometry of the river channel is a rectangular approximation.

3. Assimilation of synthetic SWOT data in ISBA/MODCOU: experimental design

3.1. The SWOT mission

The observation of water elevations from space provides important information for many physical processes in hydrology. In the continental domain, the open water surface elevations of lakes and rivers can be observed by altimetry satellites. The SWOT mission (the launch of which is expected in 2021), is a wide swath altimetry mission able to measure the spatial and temporal evolution of the open water surface elevation of oceans, lakes and reservoirs and rivers on the continental surface between 78 °S and 78 ° N (Biancamaria et al. 2016). The nominal SWOT mission lifetime is 3 years. The principal SWOT payload is the Synthetic Aperture Radar (SAR) interferometer KaRIN (Ka-band Radar Interferometer), developed at the Jet Propulsion Laboratory (JPL). The instrument has two antennas separated by a baseline distance of 10 m (Fig. 2a): by observing the same area from two different positions, the estimation of the elevation

Preprints (www.preprints.org) | NOT PEER-REVIEWED | Posted: 27 October 2018 doi:10.20944/preprints201810.0643.v1

Peer-reviewed version available at Water 2019, 11, 78; doi:10.3390/w11010078

and the position of the target can be deducted. Each swath, from either side of the nadir area, is 50 km wide and they are separated by a distance of 20 km.

The SWOT's orbit will be at a 891-km altitude, have a 77.6° inclination and function with a 21-day repeat period (the satellite flies over the same track every 21 days). Only 3.6 % of the continental surfaces between 78°S and 78°N will be never observed by SWOT (Biancamaria et al. 2016). The observed variables over continents will be open water surface elevations maps, the surface slope and the width of the river. According to Rodríguez (2016), the satellite will be designed to observe rivers wider than 100 m (requirement), with the goal being to observe rivers wider than 50 m In this study, water elevations correspond to the distance between the top of the surface water body and a reference surface, such as a geoid or an ellipsoid. The spatial resolution of the SWOT radar image in the range direction is 60 m for the near range of the swath and 10 m for the far range of the swath (Fig. 2a). It is around 5 m in the azimuth direction: the range direction is perpendicular to the propagation axis of the satellite, and the azimuth direction is parallel to the propagation axis of the satellite (Fig. 2b). At this resolution, however, vertical accuracy of the instrument could be several meters. This accuracy tends to increase when water pixels are averaged together. The requirement for the measurement is to acquire a 10 cm vertical precision on water elevation, having averaged over 1 km² of the water area (Rodríguez 2016). Measurement errors can be systematic or unsystematic. Unsystematic errors correspond to random errors (this for example is the case of errors induced by the instrument thermal noise). Systematic errors correspond to other sources of errors (such as errors induced by the atmosphere on the propagation of the signal emitted by SWOT). For many catchments in the world, only a few locations are sampled by *in situ* gauges. SWOT data will thus allow us to better understand the spatial and temporal evolution of open surface water elevations. SWOT will be the first altimetry mission to provide spatialized observations of water elevations over regional-scale basins: SWOT will observe most areas between 2 and 8 times over each 21-day period, with the number of observations primarily depending on the distance from the equator (Pavelsky et al. 2014). The Garonne catchment will be observed from 0 to 4 times per cycle, thanks to the satellite swaths, allowing several observations per cycle in most regions of the basin. However, due to these swaths overlapping, for locations with more than 1 observation per cycle, the temporal sampling between these observations will not be constant within a cycle. The number of observations inside one DA cycle however will be always the same: the distribution of the river reach observations in the catchment during one cycle will be shown in subsection 3.4.1.

3.2. Data assimilation algorithm and SWOT Observing System Simulation Experiment

The Extended Kalman Filter (EKF) was successfully employed in previous SWOT-related work from Pedinotti et al. (2014) over the Niger basin using ISBA/TRIP (Total Runoff Integrated Pathway) for model parameter correction, specifically friction coefficients. This algorithm is well adapted for weakly non-linear relation between the model outputs (noted y) and the DA control parameters to be corrected. EKF is used here over the Garonne basin to assimilate synthetic SWOT river depth observations in the RAPID module of the hydrological model ISBA/MODCOU, in order to correct Strickler coefficients K_{str} (noted x). Based on initial values of x, known as background vector x_b, the analyzed parameters x_a are calculated from Eq. 2 (Bouttier and Courtier, 1999). We call "increment" the difference in value between the background x_b and the analysis x_a.

$$x_a = x_b + (B^{-1} + HR^{-1}H^T)^{-1}H^T R^{-1}\left(y_o - H(x_b)\right) \quad (2)$$

where **B** and **R** are respectively the model error matrix and the observation model error matrix, y_o represents the observation vector (river depth or river depth difference as a function of the experiment, see results). *H* is the observation operator that maps the control vector onto the observation space, it is the composition of the hydrometeorological model integration and the extraction of output values at observation time and space. **H** is the Jacobian matrix of *H*, calculated

Preprints (www.preprints.org) | NOT PEER-REVIEWED | Posted: 27 October 2018 doi:10.20944/preprints201810.0643.v1

Peer-reviewed version available at Water 2019, 11, 78; doi:10.3390/w11010078

by using a finite difference scheme. It is a linear approximation of the observation operator H (Bouttier and Courtier, 1999).

The EKF method assumes that the system is linear. The following approximation (Eq. 3) should therefore be valid:

$$H(x + \Delta x) \approx H(x) + \frac{\partial H}{\partial x} \cdot \Delta x \quad (3)$$

In order to keep the system in the domain of the linearity, the term Δx should remain reasonably low, so that the value of the term $H(x+\Delta x)$ is nears the value of the term $H(x)+\frac{\partial H}{\partial x} \cdot \Delta x$.The higher the Δx value, the higher the difference between the left and right term of the equation. The value of Δx should be similar to the maximal difference between x_a and x_b that we decided to impose on the model, and that we call «limitation of increment».

By replacing the terms H and x in Eq. 3 to the river depth h and its argument K_{str}, we obtain the following equation (Eq. 4):

$$[h(K_{str} + \Delta K_{str})] - \left[h(K_{str}) + \frac{\partial h(K_{str})}{\partial K_{str}} \cdot \Delta K_{str}\right] = \Delta h \quad (4)$$

Δh should be equal to 0 in the case of a perfect linear model. In practice, it should remain sufficiently small to ensure good accuracy of the DA system.

OSSE are widely used to validate DA algorithms and strategies before working with real-data. They offer a convenient framework for the testing of various hypothesis on observation errors, observation spatial and temporal resolution, model error, the choice of DA algorithm or the cycling of the analysis. Knowing a SWOT's orbit and pass plan over a 21-day cycle allows the extraction of SWOT-like data from a reference simulation output of ISBA/MODCOU over the Garonne catchment. The settings of the reference simulation (noted SIM_TRUE, blue box on the top, Fig. 3) are described in Häfliger et al. (2015) and features unperturbed forcing and parameters resulting from the calibration of a RAPID model with a 1 or 2 km resolution. An error of 10 cm variance is added to the SIM_TRUE outputs to get some virtual SWOT-like observations averaged over a 1 km^2 area (blue box on the bottom, Fig. 3). This simple hypothesis will be further investigated in sub-section 4.4. A perturbed set of forcing and parameters x_b, is then used to run the background integration (noted SIM_PERT, red box, Fig. 3) in which synthetic SWOT data are assimilated in order to retrieve the unperturbed forcing and parameters. The analysis branche (noted SIM_ANA, green box, Fig. 3) for the control vector x_a allows then the calculation of the corrected parameters in order to provide corrected river depths and discharge. The DA analysis is carried out over a sliding time window covering several observation times beyond which a forecast can be issued. The tool used to set up our DA scheme is the Open-PALM (Parallel Assimilation with a Lot of Modularity) software (Fouilloux et Piacentini 1999, Buis et al. 2006) developped at CERFACS (Centre Européen de Recherche et Formation Avancée en Calcul Scientifique) and ONERA (Office National d'Etudes et de Recherches Aérospatiales). This software allows the coupling of codes of calculation between them, and in this way allows the exchange of variables such as vector or matrix between these codes. OpenPALM provides a parallel environment based on high performance implementation of the Message Passing Interface standard: this interface is able to perform both data parallelism and task parallelism (Barthélémy et al. 2017).

3.3. Sensitivity of the river depth to the roughness coefficient K_{str}

The sensitivity of the IBSA/MODCOU simulated river depth to a perturbation of the roughness coefficient K_{str} is illustrated in Fig. 4, for one unique grid cell, with typical conditions of a large rectangular plain section of the lower Garonne river. This test case is mono-dimensional, without the need to analyze the consequences of the effect of the K_{str} perturbation on the upstream and downstream river depths. Discharge Q, width W, and bed slope S_o are equal to 500 m^3 s^{-1}, 150 m and 0.0005 m m^{-1}, respectively. The K_{str} values vary between 20 and 40 m$^{1/3}$ s^{-1}. Fig. 4 shows that for a dif-

Preprints (www.preprints.org) | NOT PEER-REVIEWED | Posted: 27 October 2018 doi:10.20944/preprints201810.0643.v1

Peer-reviewed version available at Water 2019, 11, 78; doi:10.3390/w11010078

ference of K_{str} equal to 5 $m^{1/3}$ s^{-1} (between 25 and 30 $m^{1/3}$ s^{-1}), the river depth variation is about 32 cm. For a difference of 1 $m^{1/3}$ s^{-1} (between 25 and 26 $m^{1/3}$ s^{-1}), the river depth variation is about 6.5 cm. It means that an error of one Strickler coefficient equal to x_b-x_t=1 $m^{1/3}$ s^{-1} is related to an error of one river depth $H(x_b)$-$H(x_t)$=6.5 cm, x_t and $H(x_t)$ being the true Strickler coefficient and the true river depth. This result must be confirmed on the scale of the Garonne river under various hydrological conditions. In this present idealized test case considering one unique grid cell, the impact of a perturbation of K_{str} on the water level is not shown for downstream river grid cells. The results presented in section 4 allow the study of how changes in the Strickler coefficient values impact the flood dynamics on the full river network of the Garonne catchment.

In order to verify that the model is close to linearity, we undertook an experiment on a river reach located in the downstream Garonne river: Tonneins (see Fig. 1). This reach is representative of the river flows in the plain areas. The studywas set up over a period of 6 weeks (between the 15th october and 30th november 1999) with a reference K_{str} value of 30 $m^{1/3}$ s^{-1}. The chosen period experienced strong climate variability with dry and wet periods, allowing the analysis of different ranges of discharge in the selected reach. We imposed four different perturbations to the reference K_{str} value and quantified the impact on the left balance term of Eq. 4 (averaged value over the full period of study, by considering a daily time step). Table 1 shows that by comparing the 4 different perturbations, the linear approximation is only valid for small perturbations. In addition, it appears that the model is not symmetric. Hence it is important to limit the perturbations to +5 %, and to impose a maximum increment of 1.5 $m^{1/3}$ s^{-1}, in order to avoid any instability of the DA system. Table 1 shows that for a perturbation of +/- 20%, the system is not at all linear.

3.4. Data assimilation experiment setting

3.4.1. Spatial aggregation and SWOT observations

We only consider in this study that the river is over 50 m in width. Strickler coefficients K_{str} and river depths h are aggregated over 10 km reaches (5 to 10 RAPID grid cells) to meet the SWOT requirement for an observation error of 10 cm. The aggregation is operated by averaging the values in the considered grid cells, with a ponderation proportional to their length (1 or 2 km). The area of each reach varies from 0.5 to 2 km², knowing that the computed width varies from 50 m to 200 m. A total of 165 reaches (Fig. 5a) were constituted. Having to hand the orbital parameters of SWOT, a chronology of the observations for all the reaches is built over each satellite's repeat full cycle. Over the study domain in our experimental set-up, reaches are observed between 1 and 4 times per repeat period (Fig. 5b).

3.4.2. Description of the variables used in the DA platform

In the DA platform, windows with a duration of 2 to 42 days were tested, as a function of the conditions imposed in the chosen DA experiment (see section 4). The background vector x_b contains the 165 Strickler coefficient values for each river reach. The vector $H(x_b)$ contains the 165 river depths simulated by the model for each river reach. The observation vector y_o contains the p SWOT observations by a DA window. If two examples are taken with five river reaches: p=10 when these five reaches are observed 2 times during a DA window, or more complicated: p=20 when the first reach is observed 2 times, the second reach is observed 3 times, and the third, fourth and fifth reaches are observed 5 times during the window. It presents a sum of 10 SWOT observations in the first example, and 20 observations in the second. The p value is then a function of the number of SWOT passes across the catchment during one DA window, and of the number of river reaches observed during one pass of the satellite. The Jacobian matrix **H** contains the sensitivity of the 165 simulated river depths with a 5 % perturbation of the p Strickler coefficients located in the p observed reaches. The value of +5 % is chosen due to the sub-section 3.3 (see also Table 1), having a minor impact on the Δh value calculated in Eq. 4, for a typical large plain river. The observation error matrix **R** and the background error matrix **B** are diagonal: **R** contains the errors of the p river depth observations, associated with p diagonal terms. **B** contains the errors of the

Preprints (www.preprints.org) | NOT PEER-REVIEWED | Posted: 27 October 2018 doi:10.20944/preprints201810.0643.v1

Peer-reviewed version available at Water 2019, 11, 78; doi:10.3390/w11010078

165 background Strickler coefficients, associated with 165 diagonal terms. According to sub-section 3.3, in order to avoid problems of non-linearity, we decided to limit the limitation of increment to 1 $m^{1/3}$ s^{-1} in each experiment. The different variables of the Extended Kalman Filter equation (Eq. 2) and their dimension are described in Table 2.

3.4.3. Description of the data assimilation experiments

We set-up four different DA experiments (Table 3): the goal was to analyze whether or not the a priori values x_b of the Strickler coefficient could converge to a stable value and tend to the truth x_t through the assimilation windows, and if the simulated river depth $H(x_b)$ could be well estimated and tend to the true depth $H(x_t)$. The DA configuration was the same as in the previous work of Pedinotti et al. (2014) concerning the first experiment. In the three following experiments, more realistic experiments were then set up in the DA platform. In the experiments n° 1, 2 and 4, the chosen period of study is 1995-1998, and 1995-2001 in the experiment n° 3, three further years were needed in order to get a full convergence of the system. We will show that the period of study of this third experiment is longer, due to a longer convergence time of the system. During 1995 to 2001, wet and dry periods were observed. The strong climate variability of these years had a direct impact on the discharge: we consider therefore that it was a good idea to have selected these years for our test case. It allowed us to analyze a wide range of discharge signals. In the following paragraphs, a short description of all the four experiments is proposed and synthesized in Table 3.

In the first experiment, we assimilated river depths over 48 h duration windows, across a period of three years. The choice of this duration was based on one main argument: the duration corresponds to the time taken by the water to flow from the upstream to the downstream section of the Garonne river observed by SWOT, i.d. from Saint-Gaudens to Bordeaux (see Fig. 1). This means that by using a window duration of 48 hours, a roughness coefficient perturbation at Saint-Gaudens impacts all river reaches located downstream (until Bordeaux) during this window duration. It was decided that the experiment will commence with a background vector x_b initialized with values equal to 25 $m^{1/3}$ s^{-1}. This value corresponded to the averaged reference Strickler coefficient x_t in the catchment. Each diagonal term σ_B^2 of the model error matrix **B** contained values equal to the variance of all the x_b parameters around the truth x_t, with a minimum value of $(1.5\ m^{1/3}\ s^{-1})^2$. Each diagonal term σ_R^2 of the observation error matrix **R** contained values equal to $(10\ cm)^2$.

In the second experiment, we assimilated data over 48 h duration windows by perturbing the amount of runoff and drainage produced by ISBA (increasing or decreasing the production with a bias of ± 10 %), and tested the impact on the convergence through the assimilation windows. It is important to represent well the atmospheric forcing: in DA, an error of quantification or repartition of precipitations will have a direct impact on the convergence of the parameters to correct, and thus on the quality of the river flow simulation. In this way, it is important to quantify the impact of a forcing error in ISBA on the convergence of the Strickler coefficients. It was decided that the experiment should start with a background vector x_b initialized with values equal to the reference Strickler parameters on which a gaussian centered noise σ_{xb} of 5 $m^{1/3}$ s^{-1} was added. Each diagonal term σ_B^2 of the model error matrix **B** contained values equal to the variance of all the x_b parameters around the truth x_t. A minimum value of $(1.5\ m^{1/3}\ s^{-1})^2$ was imposed in the DA platform. Note than σ_{xb} was always equal to σ_B when $\sigma_B \geq 1.5\ m^{1/3}\ s^{-1}$, and $\sigma_{xb} \leq \sigma_B$ when $\sigma_B = 1.5\ m^{1/3}\ s^{-1}$. Each diagonal term σ_R^2 of the observation error matrix **R** contained values equal to $(10\ cm)^2$.

In the third experiment, river depth differences were assimilated over a 42-day duration window in the model, considering that the satellite would not observe river depths but instead, open water surface elevations. A solution for the use of water surface elevation in our system was to assimilate the water surface elevation difference δh between two consecutive observations, which was equal to river depth difference. In order to assimilate δh in the model, two or more river depth observations in one DA window were required. One can imagine two different scenarios:

1. In a DA window, there are zero or one river depth observations: It is impossible to assimilate a δh term.

Preprints (www.preprints.org) | NOT PEER-REVIEWED | Posted: 27 October 2018 doi:10.20944/preprints201810.0643.v1

Peer-reviewed version available at Water 2019, 11, 78; doi:10.3390/w11010078

2. In a DA window, there are n observations ($n \geq 2$): It is possible to assimilate n-1 δh terms

In order to respect the case n° 2 for all reaches of the Garonne basin, we decided to extend the assimilation window to 42 days, to be sure that at least two observations were present for each reach in the assimilation window. It was decided to start the experiment with a background vector x_b initialized with values equal to the reference Strickler parameters on which a gaussian centered noise σ_{xb} of 5 $m^{1/3}$ s^{-1} was added. Each diagonal term σ_B^2 of the model error matrix **B** contained values equal to the variance of all the x_b parameters around the truth x_t. A minimum value of (2.12 $m^{1/3}$ s^{-1})^2 was imposed in the DA platform. Each diagonal term σ_R^2 of the observation error matrix **R** contained values equal to (14.1 cm)^2.

In the fourth experiment, we increased the realism of the SWOT error measurement, by implementing time-and-space variable errors of observation: each diagonal term σ_R^2 of the observation error matrix **R** contained values varying for every reach at each DA window. Data were assimilated over a 48 h duration window. The decision was made to start the experiment with a background vector x_b initialized with values equal to the reference Strickler parameters on which a gaussian centered noise σ_{xb} of 5 $m^{1/3}$ s^{-1} was added. Each diagonal term σ_B^2 of the model error matrix **B** contained values equal to the variance of all the x_b parameters around the truth x_t. A minimum value of (1.5 $m^{1/3}$ s^{-1})^2 was imposed in the DA platform.

Note that the common criterion for the comparison of these 4 different DA experiments, is the quality of the convergence of the Strickler coefficients K_{str} to the truth x_t. The convergence time of the K_{str} is irrelevant for the comparison between the 4 experiments, because the duration of the DA windows, the first guess x_b of the K_{str} at the beginning of the experiment, and the attribution of the diagonal terms in the R and B matrices vary in function to the experiment.

4. Results

4.1. Assimilation of river depths (experiment 1)

We decided in this first DA experiment to impose a minimum value of the diagonal terms σ_B^2 in the **B** matrix to (1.5 $m^{1/3}$ s^{-1})^2: When the values are too low (< (1 $m^{1/3}$ s^{-1})^2), the convergence of the terms (x_b-x_t) to the truth x_t is complicated, because the analysis is closer to the background than the observation (for the EKF, there are fewer uncertainties in the background than in the observation). This limitation criterion improves thus the convergence of the terms (x_b-x_t) to the truth x_t. Concerning the value of the increment (x_a-x_b), when no limitation is imposed, the values of the terms (x_b–x_t) of the DA system are very high in the first windows (between -40 to +70 $m^{1/3}$ s^{-1}), and the convergence time is about 800 days. When a limitation of increment of 5$m^{1/3}$ s^{-1} is imposed, the values of the terms (x_b–x_t) of the DA system during the early windows are between -40 and +30$m^{1/3}$ s^{-1}until 100 days of assimilation, and the convergence to the truth occurs after 240 days. In the current experiment illustrated in Fig. 6, the majority of the K_{str} values converge to the truth after 700 days of assimilation, considering a limitation of increment fixed to 1 $m^{1/3}$ s^{-1}. We consider that the Strickler coefficient convergence to the truth x_t is reached when the standard deviation σ_{xb} between all (x_b-x_t) values is equal or lower than 1 $m^{1/3}$ s^{-1}.

In Fig. 7, we show the analyzed and the true river depth for the reaches of Lamagistère (a) and Bergerac (b) located respectively in the downstream Garonne and Dordogne river (see Fig. 1). We have chosen these two reaches firstly because they are representative of plain rivers where SWOT will provide observations, and secondly because their initial Strickler coefficient in the DA system is far from the truth x_t.

At Lamagistère, the initial value was 25 $m^{1/3}$ s^{-1}, while the true value was 38.7 $m^{1/3}$ s^{-1}. The simulated river depth $H(x_b)$ was then higher than the true river depth $H(x_t)$, with a positive difference of about 20 cm in normal flow, and more than 80 cm during flood periods. The average true river depth $H(x_t)$ over the full period of study (365 days) was equal to 2.11 m, with peak values up until 7.5 m. Furthermore at the beginning of the experiment, the river flow velocity at

Preprints (www.preprints.org) | NOT PEER-REVIEWED | Posted: 27 October 2018 doi:10.20944/preprints201810.0643.v1

Peer-reviewed version available at Water 2019, 11, 78; doi:10.3390/w11010078

Lamagistère and upstream was too low (due to low x_b values compared to x_t): the temporal delay between the analyzed river depth time series and the true time series was negative (about one day of delay).

At Bergerac, the case was the opposite: we started the experiment with a Strickler coefficient value higher than the truth x_t (positive difference of 7.5 $m^{1/3}$ s^{-1}) which was equal to 17.5 $m^{1/3}$ s^{-1}: the relative difference between the first x_b value and x_t was equal to +42.9 %. The simulated river depth $H(x_b)$ was then higher than the true river depth $H(x_t)$, with a negative difference of 20-30 cm in normal flow, and more than 1 m during flood periods. The average true river depth $H(x_t)$ over the full period of study (365 days) was equal to 2.10 m, with peak values up to 9 m. Furthermore at the beginning of the experiment, the river flow velocity at Bergerac and upstream was too high (due to high x_b values compared to x_t): the delay between the analyzed river depth time series and true time series was positive (with about one day of advance).

For Lamagistère and Bergerac after 365 days of assimilation, both the phasing and signals between $H(x_b)$ and $H(x_t)$ were improved: the time difference between the arrival of one $H(x_b)$ peak and one $H(x_t)$ peak was less than 3 hours, and the difference between $H(x_b)$ and $H(x_t)$ was inferior to 10 cm for every discharge regime.

4.2. Assimilation of river depths, in case of atmospheric forcing biases (experiment 2)

In this experiment, we propose two different scenarios. In the first (a), the water produced by ISBA (runoff+drainage) is decreased by 10 %. In the second scenario (b), the water produced by ISBA is increased by 10 %. The main goal of the experiment is to analyze what the impact of these errors on the Strickler coefficient convergence is. The effect of the over-production of water in the river is the following: the DA system will tend to increase the K_{str} values in order to decrease the river depth. The effect of an under-production of water in the river is the opposite: the DA system will decrease the K_{str} values in order to increase the river depth. The illustration in Fig. 8 shows that after about 1000 days of assimilation, the Strickler coefficient values converge to a stable state, but differ from the true x_t with an average bias of -1.56 $m^{1/3}$ s^{-1} in the scenario (a), and an average bias of +1.83 $m^{1/3}$ s^{-1} in the scenario (b). For water production bias of +10 % or -10 %, we showed that the impact on the terms (x_b-x_t) at the end of the DA experiment was inferior to 2 $m^{1/3}$ s^{-1}, having a minor impact on the flow velocity (phasing delay of 3 hours at Tonneins between the «true» hydrograph and the «analyzed» hydrograph).

4.3. Assimilation or river depth differences (experiment 3)

The variance of the observation error for two consecutive observations h_t and h_{t+1} follows Eq. 5:

$$Var(h_{t+1} - h_t) = Var(h_t) + Var(h_{t+1}) - 2cov(h_t, h_{t+1}) \quad (5)$$

Assuming that two consecutive observation errors are not correlated and that the SWOT error is 10 cm (standard deviation), cov(h_t, h_{t+1})=0 and the observation error $(Var(h_{t+1}-h_t))^{1/2}$ becomes thus σ_R=14.1 cm.

In order to keep the same ratio between the diagonal term σ_R and σ_B (see Eq. 6) of the two matrix **R** and **B** (as the experiments detailed in the sub-sections 4.1 and 4.2), the minimum value of σ_B is now fixed to 2.12 $m^{1/3}$ s^{-1}. This value is calculated from the diagonal terms σ_B equal to 1.5 $m^{1/3}$ s^{-1} in the **B** matrix used in the two previous experiments. We show in Fig. 9 the temporal evolution of the terms (x_b-x_t) for all reaches in the basin.

$$\frac{\sigma_{R(exp1)}}{\sigma_{B(exp1)}} = \frac{\sigma_{R(exp3)}}{\sigma_{B(exp3)}} \rightarrow \sigma_{B(exp3)} = \sigma_{R(exp3)} \cdot \frac{\sigma_{B(exp1)}}{\sigma_{R(exp1)}} \quad (6)$$

After 15 DA windows (2 years or 750 days), the majority of the Strickler coefficients in the DA system converged to the truth x_t. The convergence of 4 reaches occur more slowly: one plausible hypothesis is that the observation error is on average larger than for the other reaches, driven by the random gaussian noise σ_R which can be lower or higher than 14.1 cm across the full study period. There are only 50 DA windows in this experiment, and the impact of σ_R on the convergence of x_b is different for one given reach after these 50 windows, when the experiment is remade. After 50

Preprints (www.preprints.org) | NOT PEER-REVIEWED | Posted: 27 October 2018 doi:10.20944/preprints201810.0643.v1

Peer-reviewed version available at Water 2019, 11, 78; doi:10.3390/w11010078

windows or 2100 days of assimilation, the standard deviation σ_{xb} of all (x_b-x_t) terms is about 1.70 $m^{1/3}$ s^{-1}: this value is bigger than the σ_{xb} value presented in the first experiment (sub-section 4.1), because the diagonal terms σ_R^2 and σ_B^2 imposed in the observation error matrix **R** and the model error matrix **B** are more significant.

4.4. Assimilation of river depths considering more realistic SWOT errors (experiment 4)

In this last experiment, the objective is to evaluate the impact of the introduction of slightly more realistic SWOT observation errors, derived (but still simplified) from some technical characteristics of the mission on the assimilation DA platform.

In this experiment, the diagonal terms σ_R in the observation error matrix **R** vary in space and time (at each DA window). The total error (taking into account the variable and constant errors averaged in time and space) should be equal to 10 cm, and is composed of systematic and non-systematic errors (Rodríguez 2016). The non-systematic errors are random and gaussian, and the systematic errors are constant (see sub-section 3.1). We are able to approximate by a very simple method the different sources of instrumental error contributing to the changing of the SWOT error measurement values in space and time. 4 factors with an impact on the diagonal term values σ_R of the observation error matrix **R** are introduced, allowing σ_R to vary at each time step and for every river reach. The first three factors (non-systematic source of errors) are: the surface of the reach, the SWOT look angle and the radar water surface roughness. The calculation of these simple instrumental-like errors is based on the previous works of Enjolras et al. (2006). The last factor having an impact on the σ_R of the **R** matrix is the wet-troposphere error (systematic source of errors). This error is estimated in this study by the intra-day variability of water content in the troposphere. There are other sources of errors, more difficult to quantify, but they should have a lower impact on the total error budget at the reach scale: they are the ionosphere signal, the dry troposphere signal, the orbit radial component, and the KaRIn random and systematic errors after cross-over corrections. Table 4 summarizes the SWOT error budget (Brown and Obligis, 2014), after averaging a 1 km² area (Rodríguez 2016). It is important to note that all the equations used to calculate these different sources of instrumental errors are greatly simplified, the more realistic and complex full radar equations are not used in our study. The main goal of this fourth experiment is to take into account errors of measurement more realistic than simple gaussian errors of 10 cm, but it is important to keep in mind that these errors are simplified compared to the detailed error budget calculated by the SWOT simulator used by the JPL and the CNES (see Fernandez et al. 2017).

4.4.1. SWOT instrumental error along the swath

The SWOT error measurement is linked to the surface of the observed reach: it is a non-systematic source of error. When several raw SWOT radar images are averaged over a bigger area, the error decreases with the squared root of the number of raw SWOT radar images (Rodríguez 2016). The surface of the reach is proportional to the width *W*. When the river width decreases, the error increases because the observed surface by the satellite is lower. Furthermore, the measurement errors increase with the look angle of the satellite because the surface of the raw SWOT radar image is not the same: 70m x 5m for the far range image, and 10 m x 5 m for the near range image (see sub-section 3.1). These measurement errors then vary along the swath. Based on the works of Enjolras et al. (2006) who developed a simple algorithm calculating the sensitivity of the measurement error as a function of the river width and the look angle of the satellite. The SWOT look angle will vary from 0.6° to 4.3°, corresponding respectively to the inner and outer board of each swath.

The roughness of the open water surface will determine the amount of energy reflected to the satellite and will thus impact SWOT's error budget. In our case study, the roughness is simulated very simply, considering that it depends only on the wind velocity, and was previously validated over the ocean domain only (see Enjolras et al. 2006). Even if the important complexity of these sources of errors is not well taken into account, the goal for our study is to consider the

Preprints (www.preprints.org) | NOT PEER-REVIEWED | Posted: 27 October 2018 doi:10.20944/preprints201810.0643.v1

Peer-reviewed version available at Water 2019, 11, 78; doi:10.3390/w11010078

main processes and to understand how the measurement errors vary along the swath. On Fig. 10, we show the sensitivity of the error we considered in our study to the wind speed near the water surface (based on the works of Enjolras et al. (2006)), considering a river reach of 10 km long and 100 m wide. Over the full period 01/08/1995 – 31/07/1998, 75 % of the wind speed values are between 0 and 3 m s^{-1}. Wind speed values higher than 8 m s^{-1} are rare, representing about 1 % of all wind speed values over the study period. The wind speeds correspond to SAFRAN reanalysis data at 10 m (3-hour time step) averaged over a 10 minute period.

4.4.2. The intra-day variability of water content in the troposphere: impact on the SWOT error of measurement

According to Brown and Obligis (2014), the estimation of the wet troposphere error is about 4 cm (Table 4). Water content changes in the troposphere have a direct impact on the velocity of electromagnetic waves. Numerical atmospheric models are able to produce a correction of the wet troposphere error. The water content simulated by models in the atmosphere however also shows an error. Several studies looked at the impact of errors in meteorological model outputs or in in situ observations concerning the representation of water content in the troposphere (Cimini et al. 2012, Ning et al. 2013): these errors of the atmospheric state should be taken into account, in order to determine the error on the measured open water surface elevation. We would like to base our study on the previous works of Flentje et al. (2007) who showed that it is more difficult to quantify the water content in a transition meteorological period than during a stable period: we have defined a transition period equivalent to an interval of time with an important variability of the troposphere state, and a stable period equivalent to an interval of time with a low variability of the troposphere state. The variable chosen to describe this temporal variability is the water content, and the chosen interval of time is 24 hours: this time value is well representative of the meteorological variability, especially in summer with important changes of the troposphere state during a full 24-hour period (important contrasts between day and night). The SAFRAN reanalysis data of water content (g kg^{-1}) at 10 m (3-hour time step) are used to calculate intra-day variances *Vi* (g $kg^{-1})^2$ across the study period 01/08/1995 – 31/07/1998. Taking into account the 165 river reaches of the DA platform over the full study period, a simple relationship between the intra-day variance of water content *Vi* and the SWOT error measurement σ_R is set up: the greater *Vi*, the greater the measurement error. We would like to build a linear relationship between *Vi* and σ_R. Once the relationship between *Vi* and σ_R is established, one can attribute a SWOT error measurement error σ_R at each time step for every river reach of the catchment. The slope of the function linking *Vi* and σ_R is equal to 6.67 cm/(g $kg^{-1})^2$. This relationship is based on the assumption that the spatial and temporal averaged wet troposphere error is equal to 4.0 cm (see Table 4), and that the full spatio-temporal SAFRAN reanalysis data distribution of water content is well-known in each river grid cell of the catchment. 80 % of the *Vi* values range between 0 and 1 (g $kg^{-1})^2$. Values higher than 3 (g $kg^{-1})^2$ are rare, representing about 1 % of all *Vi* values over the full study period.

4.4.3. SWOT DA experiment using realistic errors of measurement

Taking into account the sensitivity of the SWOT measurement error to the two described errors in the sub-section 4.4.1 and 4.4.2, it is possible to conduct this last experiment with slightly more realistic errors. The observation error matrix **R** is built taken into account the two sources of errors described in sub-sections 4.4.1 and 4.4.2: each term σ_R varies at each time step of the experiment for every river reach, and the spatio-temporal average of σ_R over the full period of study and domain is equal to 10 cm. After 365 days of assimilation, the majority of the parameters converges to the truth x_t with a standard deviation of ~1 $m^{1/3}$ s^{-1}.During the DA windows n° 259 and 448, and 518 and 896 days of assimilation, the standard deviation σ_{xb} between all (x_b-x_t) values decreases respectively to 0.76 and 0.79$m^{1/3}$ s^{-1}(Fig. 11). To understand these low values, we analyzed the temporal evolution of the *Vi* variable over the full study period: it showed that during the winter months the values of *Vi* are equal to 0.5 (g $kg^{-1})^2$ on average (the days 518 and 896 of this experiment are in the winter season), and 1.5 (g $kg^{-1})^2$ on average during the summer months. The low values of *Vi* during the

Preprints (www.preprints.org) | NOT PEER-REVIEWED | Posted: 27 October 2018 doi:10.20944/preprints201810.0643.v1

Peer-reviewed version available at Water 2019, 11, 78; doi:10.3390/w11010078

winter season lead to low SWOT error measurements σ_R, and then to a better convergence of the K_{str} values to the truth x_t. The convergence time of this DA experiment is around 600 days when the x_b values of each reaches converge at the truth x_t.

5. Conclusion and perspectives

This study is a contribution to the building of a DA scheme over the Garonne basin within the framework of the SWOT mission. More precisely, the objective of this study has been to evaluate the ability of a regional hydrometeorological model in order to assimilate synthetic SWOT river depths in the Garonne catchment, and to correct the Strickler roughness coefficient K_{str} of the river bed.

In every experiment, we showed the ability of the DA system to calibrate the K_{str}parameter around the known truth. In the first experiment, we showed that the parameters converge to the truth after ~ 2 years, with an average error of ±1 $m^{1/3}$ s^{-1}, and with an associated average error on river depths of ±5 cm. The choice of the maximum increment value (the difference between the analysis x_a and the a priori value of the Strickler coefficient x_b) has an impact on the time of convergence. In the second experiment, we showed the importance of the atmospheric forcing and its impact on the convergence of the K_{str} parameters. An error of ±10 % water produced by ISBA lead to an error of ±1.5 $m^{1/3}$ s^{-1}, but had a minor impact on the river flows. The impact of greater errors on the discharge phasing should be taken in consideration. The third experiment illustrated the interest of assimilating the difference of river depths instead of absolute open surface water elevations that are equivalent to river depths in our study. The bathymetry elevation is unknown in RAPID, and the satellite will not provide measurements of river depths. The duration of a DA window should be equal to 42 days, in order to be sure that every reach is observed at least two times twice during one DA window. The quality of the convergence (±1.69 $m^{1/3}$ s^{-1}) is slightly lower in comparison with the first experiment, but the time of convergence is equivalent (~ 2 years). In the last experiment, we proposed the introduction of more realistic SWOT error measurements varying in time and space, which depend on the surface of the observed reach, the look angle of the satellite, the surface water roughness, and the intra-day variability of the water content in the troposphere. The impact of the last factor seems to play an important role: the convergence is on average better during the winter months than during the summer months, because of a low temporal variability of the troposphere water content.

Several points concerning data assimilation in the context of the SWOT mission could be explored. The four main ones are as follow:

5.1. The choice of the data assimilation method and the experimental design

The main goal of each presented experiment in section 4 was to calibrate the Strickler coefficients in order to converge them to the truth, in the context of twin experiments. The choice of the EKF requires the use of the hydrological river routing model RAPID in the domain of the linearity: it has its limitations: the perturbation of the parameters we want to correct (roughness coefficient) should be small, they require limited increment values (a maximum difference between the first guess x_b and the analysis x_a calculated by the DA system). Other methods such as the Ensemble Kalman Filter (EnKF) (Evensen 2004) could be tested to see whether or not it is possible to reduce the convergence time of the parameters, or to decrease the standard deviation σ_{xb} around the truth x_t at the end of one given DA experiment. In our study, we assume that the model is linear: we should use it in the domain of linearity by imposing small perturbations to the parameter to correct. The EnKF can be used in the domain of non-linearity and could be tested. It has gained popularity because of its simple conceptual formulation and relatively easy implementation, requiring no derivation of a tangent linear operator or adjoint equations, and no integrations backward in time (Evensen 2004). Concerning the description of the different variables and data assimilation experiments described in the sub-section 3.4, other way in which to build the experimental design could be proposed: one important one is the testing of what the impact is on different

Preprints (www.preprints.org) | NOT PEER-REVIEWED | Posted: 27 October 2018 doi:10.20944/preprints201810.0643.v1

Peer-reviewed version available at Water 2019, 11, 78; doi:10.3390/w11010078

lengths of river reaches on the convergence of the Strickler coefficients in all four DA experiments, the SWOT error measurement being directly linked to the length of the reaches. Another point is the attribution of the different parameters used in the DA platform: choice of the DA window duration, threshold of the increment (x_a-x_b) limitation, and attribution of the model error matrix. The choice of the attribution of the first a priori value x_b at the beginning of each experiment also plays an important role, having a direct impact on the time of convergence of the Strickler coefficients. The study period can present a more or less spatial and temporal variability of precipitations reaching the surface, impacting directly the flood dynamics in the river network, and thus the increment term (x_a-x_b) which depends on the discharge regime. All these factors shortly described could have different impacts on the convergence of the system.

5.2. Choice of the observation to assimilate and the parameter to correct

In the study, we decided to assimilate synthetic SWOT river depths in order to calibrate the roughness coefficient of the river bed in the Garonne catchment. The possibility to assimilate river widths or water surface bed slopes should be investigated. In our work, we considered that the river channel geometry is rectangular and that the width is thus constant in time in each river grid cell. In reality, the amplitudes of the river width between summer (low discharge) and winter (high discharge) can be several tens of meters. The implementation of a trapezoidal geometry should be investigated, in order to take into account the temporal variability of the river width. Furthermore, instead of a parameter calibration, one could propose the correction of the state of prognostic variables in RAPID (initial water volumes in the river reach) or in ISBA (soil water content), or the correction of the description of the atmospheric forcing SAFRAN. Thirel et al. (2008) proposed the assimilation of discharge over France in ISBA/MODCOU, in order to correct the initial value of the soil moisture. This kind of study could also be realized with synthetic river depths instead of discharge. The correction of prognostic variables instead of parameters could lead to significant advances for operational hydrology, such as the monitoring of water resources and better representation of floods on a regional scale.

5.3. Assimilation of river depths considering more realistic SWOT errors

In the last proposed DA experiment (sub-section 4.4), we decided to set up a more realistic scheme leading to a better representation of the SWOT error measurements. Several points can be considered. The dependence of the error to the reach surface is well established by Rodríguez (2016), but other factors could have an important impact on the measurement error, like the presence of topography and/or vegetation around the reach, or the orientation of the reach compared to the azimuthal direction of the satellite: the area of the SWOT raw radar image is not the same as a function of the propagation direction of the satellite, and it will be therefore possible to aggregate more or fewer raw radar images over a 1 km² water area; only the non-systematic errors are impacted by this last factor. They should be taken into account in order to better quantify the measurement error. But to do so, a more complex SWOT simulator is required: the high resolution SWOT hydrology simulator (https://swot.jpl.nasa.gov/) will allow a better quantification of the error than in the present study. This simulator is currently used at fine spatial and temporal scales in comparison with those used in this study. It would be interesting to test whether or not it works on a regional or global scale or, based on the results from this simulator, whether or not it will be possible to parametrize SWOT errors in a more realistic way than what has been achieved in this study.

Concerning the wet tropospheric signal, the chosen criterion was the intra-day variability *Vi* of the water content at 10 m. We showed that this variability is greater in summer than in winter, and proposed that the associated measurement error is proportional to *Vi*. We assumed in this way that it is more difficult to represent variable states than stable states of the troposphere in the time. This hypothesis needs more investigation by considering carefully the synoptic weather situation. For example, important changes of water content due to a warm or cold front (case A) are more difficult to represent than the diurnal temporal evolution of the water content in a homogeneous synoptic situation (case B), be-

Preprints (www.preprints.org) | NOT PEER-REVIEWED | Posted: 27 October 2018 doi:10.20944/preprints201810.0643.v1

Peer-reviewed version available at Water 2019, 11, 78; doi:10.3390/w11010078

cause there may be uncertainties about the arrival time of the front: a *Vi* value of 1 $(g\ kg^{-1})^2$ could be therefore more difficult to estimate in case A than the same *Vi* value during case B.

5.4. Extension of SWOT DA in other catchments of the world

The main perspective of this study is to extend the assimilation of SWOT observations not only across the Garonne basin, but all over the world where observations are available. The initial decision to use SRTM 90 m (Farr et al. 2007) as a Digital Elevation Model (DEM) will make this operation possible. Finally, the use of real satellite data (e.g. altimetry nadir JASON-2/-3, ENVISAT or SARAL, Sentinel-3) could be tested over big river basins such as the Amazon or the Congo basin, and will allow inter-comparisons between actual experiments and our SWOT twin experiments.

References

Alkama, R. and co-authors, 2010: Global evaluation of the ISBA-TRIP continental hydrological system. Part I: Comparison to GRACE terrestrial water storage estimates and in situ river discharges, *Journal of Hydrometeorology*, 11, 583-600.

Alsdorf, D. E., E. Rodríguez and D. P. Lettenmaier (2007): Measuring surface water from space, Rev. Geophys., 45, 1-24.

Barthélémy, S., S. Ricci, M.C. Rochoux, E. Le Pape and O. Thual (2017): Ensemble-based data assimilation for operational flood forecasting – On the merits of state estimation for 1D hydrodynamic forecasting through the example of the "Adour Marine" river, *Journal of Hydrology*, 552, 210-224.

Biancamaria, S., K. M. Andreadis, M. Durand, E. A. Clark, E. Rodríguez, N. M. Mognard, D. E. Alsdorf, D. P. Lettenmaier and Y. Oudin (2010): Preliminary characterization of SWOT hydrology error budget and global capabilities, *IEEE Journal of Selected Topics in Applied Earth Observations and Remote Sensing*, 3, 6-19.

Biancamaria, S., M. Durand, K. M. Andreadis, P. D. Bates, A. Boone, N. M. Mognard, E. Rodríguez, D. E. Alsdorf, D. P. Lettenmaier and E. A. Clark. (2011): Assimilation of virtual wide swath altimetry to improve Arctic river modeling, *Remote Sensing of Environment*, 115, 373-381.

Biancamaria, S. D. P. Lettenmaier and T. M. Pavelsky (2016): the SWOT mission and Its capabilities for land hydrology, *Surveys in Geophysics, 37, 307-337, doi:10.1007/s10712-015-9346-y.*

Bouttier, F. and P. Courtier (1999): Data assimilation concepts and methods, *ECMWF Lecture Note*.

Brown S. and E. Obligis (2014): SWOT Wet Tropospheric Correction Working Group Report, 3rd SWOT Science Defintion Team meeting, 14-16 January 2014, Washington DC, USA.

Buis, S., A. Piacentini and D. Déclat (2006): PALM: A Computational framework for assembling high performance computing applications, *Concurrency Computat, Pract. Exper.*, 18, 247-262.

Cimini D., N. Pierdicca, E. Pichelli, R. Ferretti, V. Mattioli, S. Bonafoni, M. Montopoli and D. Perissin: On the accuracy of integrated water vapor observations and the potential for mitigating electromagnetic path delay error in InSAR, *Atmos. Meas. Tech.*, 5, 1015-1030.

Caballero, Y., Voirin-Morel, S., Habets, F., Noilhan, J., Le Moigne, P., Lehenaff, A., Boone, A.: Hydrological sensitivity of the Adour-Garonne river basin to climate change, Water Resources Research, 43, W07448, doi:10.1029/2005WR004192, 2007.

David, C.H., Habets, F., Maidment, D.R. and Yang, Z-L (2011a): RAPID applied to the SIM France model, *Hydrol. Process.*, 25, 3412– 3425.

David, C.H., D. R. Maidment, G.-Y. Niu, Z.-L. Yang, F. Habets and V. Eijkhout (2011b): River network routing on the NHDPlus dataset, *Journal of Hydrometeorology*, 12, 913-934.

Preprints (www.preprints.org) | NOT PEER-REVIEWED | Posted: 27 October 2018 doi:10.20944/preprints201810.0643.v1

Peer-reviewed version available at Water 2019, 11, 78; doi:10.3390/w11010078

Decharme B., R. Alkama, H. Douville, M. Becker and A. Cazenave (2010): Global Evaluation of the ISBA−TRIP Continental Hydrological System. Part II: Uncertainties in River Routing Simulation Related to Flow Velocity and Groundwater Storage, *J. Hydrometeor*, 11, 601−617.

Emery, C. M., S. Biancamaria, A. Boone, P.-A. Garambois, and B. Decharme (2016): Temporal Variance-Based Sensitivity Analysis of the River-Routing Component of the Large-Scale Hydrological Model ISBA-TRIP: Application on the Amazon Basin, *J. Hydrometeor*, 17(2).

Enjolras, V., P. Vincent, J.-C. Souyris, E. Rodríguez, L.Phalippou and A. Cazenave (2006): Performances study of interferometric radar altimeters: from the instrument to the global mission definition, *Sensors*, 6, 164-192.

Farr, T. G., P. A. Rosen, E. Caro, R. Crippen, R. Duren, S. Hensley, M. Kobrick, M. Paller, E. Rodríguez, L. Roth, D. Seal, S. Shaffer, J. Shimada, J. Umland, M. Werner, M. Oskin, D. Burbank and D. Alsdorf (2007): The Shuttle Radar Topography Mission, Rev. Geophys., 45, 1-33.

Faroux, S., A. T. Kaptué Tchuenté, J.-L. Roujean, V. Masson, E. Martin and P. Le Moigne (2013): ECOCLIMAP-II/Europe: a twofold database of ecosystems and surface parameters at 1 km resolution based on satellite information for use in land surface, meteorological and climate models, *Geosci. Model Dev.*, 6, 563-582.

Fernandez, D.E. (2017): SWOT Project, Mission performance and error budget, JPL document D-79084, Rev. A, https://swot.oceansciences.org/docs/SWOT_D-79084_v10Y_FINAL_REVA__06082017.pdf.

Flentje, H., A. Dörnbrack, A. Fix, G. Ehret and E. Holm (2007): Evaluation of ECMWF water vapour fields by airborne differential absorption lidar measurements: a case study between Brazil and Europe, *Atmos. Chem. Phys.*, 7, 5033-5042.

Fouilloux, A. and A. Piacentini (1999): The PALM Project: MPMD Paradigm for an Oceanic Data Assimilation Software, *Lectures Notes In Computer Science*, 1685, 1423-1430.

Goutal, N. and F. Maurel (2002): A finite volume solver for 1D shallow water equations applied to an actual river, *Int. J. Numer. Meth. Fluids*, 38, 1–19.

Häfliger, V. E. Martin, A. Boone, F. Habets, C. H. David, P.-A. Garambois, H. Roux, S. Ricci, L. Berthon, A. Thévenin and S. Biancamaria (2015): Evaluation of Regional-Scale River Depth Simulations Using Various Routing Schemes within a Hydrometeorological Modeling Framework for the Preparation of the SWOT Mission, *Journal of Hydrometeorology*, 16, 1821-1842.

Larnier, K. (2010): Modélisation thermohydraulique d'un tronçon de Garonne en lien avec l'habitat piscicole: approches statistique et déterministe, *thèse de doctorat*, Université de Toulouse, France.

Ledoux, E., G. Girard and J.P. Villeneuve (1984): Proposition d'un modèle couplé pour la simulation conjointe des écoulements de surface et des écoulements souterrains sur un bassin hydrologique. *La Houille Blanche*: 101-110.

Ledoux, E., G. Girard, G. D. Marsily and J. Deschenes (1989): Spatially distributed modelling: Conceptual approach, coupling surface water and ground-water, in Unsaturated Flow in Hydrologic Modelling: Theory and Practice, NATO ASI Ser. C, edited by H. J. Morel-Seytoux, pp. 435–454, *Kluwer Acad., Norwell, Mass.*

Masson, V., P. Le Moigne, E. Martin, S. Faroux, A. Alias, R. Alkama, S. Belamari, A. Barbu, A. Boone, F. Bouyssel, P. Brousseau, E. Brun, J.-C. Calvet, D. Carrer, B. Decharme, C. Delire, S. Donier, K. Essaouini, A.-L. Gibelin, H. Giordani, F. Habets, M. Jidane, G. Kerdraon, E. Kourzeneva, M. Lafaysse, S. Lafont, C. Lebeaupin Brossier, A. Lemonsu, J.-F. Mahfouf, P. Marguinaud, M. Mokhtari, S. Morin, G. Pigeon, R. Salgado, Y. Seity, F. Taillefer, G. Tanguy, P. Tulet, B. Vincendon, V. Vionnet and A. Voldoire (2013): The SURFEX v7.2 land and ocean surface platform for coupled or offline simulation of earth surface variables and fluxes, *Geosci. Model Dev.*, 6, 929-960.

Ning, T., G. Elgered, U. Willen and J.M. Johansson (2013): Evaluation of the atmospheric water vapor content in a regional climate model using ground-based GPS measurements, *Journal of Geophysical Research*: Atmosphere, 118, 329-339.

Preprints (www.preprints.org) | NOT PEER-REVIEWED | Posted: 27 October 2018 doi:10.20944/preprints201810.0643.v1

Peer-reviewed version available at Water 2019, 11, 78; doi:10.3390/w11010078

Noilhan, J. and S. Planton (1989): A simple parameterization of land surface processes for meteorological models, *Monthly Weather Review*, 117, 536–549.

Pavelsky, P., M. Durand, K. M. Andreadis, R. E. Beighley, R. C. D. Paiva, G. H. Allen and Z. F. Miller (2014): Assessing the potential global extent of SWOT river discharge observations, *Journal of Hydrology*, 519, 1519-1525.

Pedinotti, V., A. Boone, B. Decharme, J.F. Crétaux, N. Mognard, G. Panthou, F. Papa and B.A. Tanimou (2012): Evaluation of the ISBA-TRIP continental hydrological system over the Niger basin using in situ and satellite derived datastes, *Hydrology and Earth System Sciences*, 16, 1745-1773.

Pedinotti, V., S. Ricci, S. Biancamaria and N. Mognard (2014): Assimilation of satellite data to optimize large scale hydrological model parameters: A case study for the SWOT mission, *Hydrol. Earth Syst. Sci.*, 18, 4485–4507.

Rodríguez, E. (2016): Surface Water and Ocean Topography (SWOT), Science Requirements Document, JPL document D-61923, Rev. A, http://swot.jpl.nasa.gov/files/swot/D-61923_SRD_Rev%20A_20160318%20with%20signatures1.pdf.

Santos da Silva, J., S. Calmant, F. Seyler, O. Corrêa Rotunno Filho, G. Cochonneau and W. João Mansur (2010): Water levels in the Amazon basin derived from the ERS2 and ENVISAT radar altimetry missions, *Remote sensing of Environment*, 114, 2160-2181.

Thirel, G., E. Martin, J.-F. Mahfouf, S. Massart, S. Ricci and F. Habets (2010): A past discharge assimilation system for ensemble streamflow forecasts over France – Part 1: Description and validation of the assimilation system, *Hydrol. Earth Syst. Sci.*, 14, 1623-1637, doi:10.5194/hess-14-1623-2010

Zaitchik, B. F., M. Rodell and R. H. Reichle (2008): Assimilation of GRACE Terrestrial Water Storage Data into a Land Surface Model: Results for the Mississippi River Basin, *Journal of Hydrometeorology*, 9, 535-548

Preprints (www.preprints.org) | NOT PEER-REVIEWED | Posted: 27 October 2018 doi:10.20944/preprints201810.0643.v1

Peer-reviewed version available at *Water* **2019**, *11*, 78; doi:10.3390/w11010078

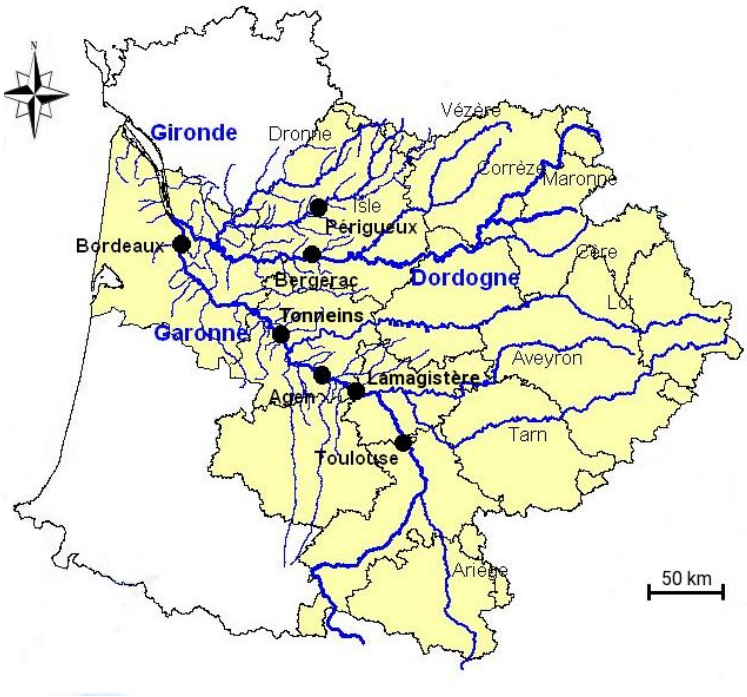

Figure 1: The Garonne catchment with the names of main rivers (blue) and tributaries (black), and the names of main cities (dark black)

Preprints (www.preprints.org) | NOT PEER-REVIEWED | Posted: 27 October 2018 doi:10.20944/preprints201810.0643.v1

Peer-reviewed version available at Water 2019, 11, 78; doi:10.3390/w11010078

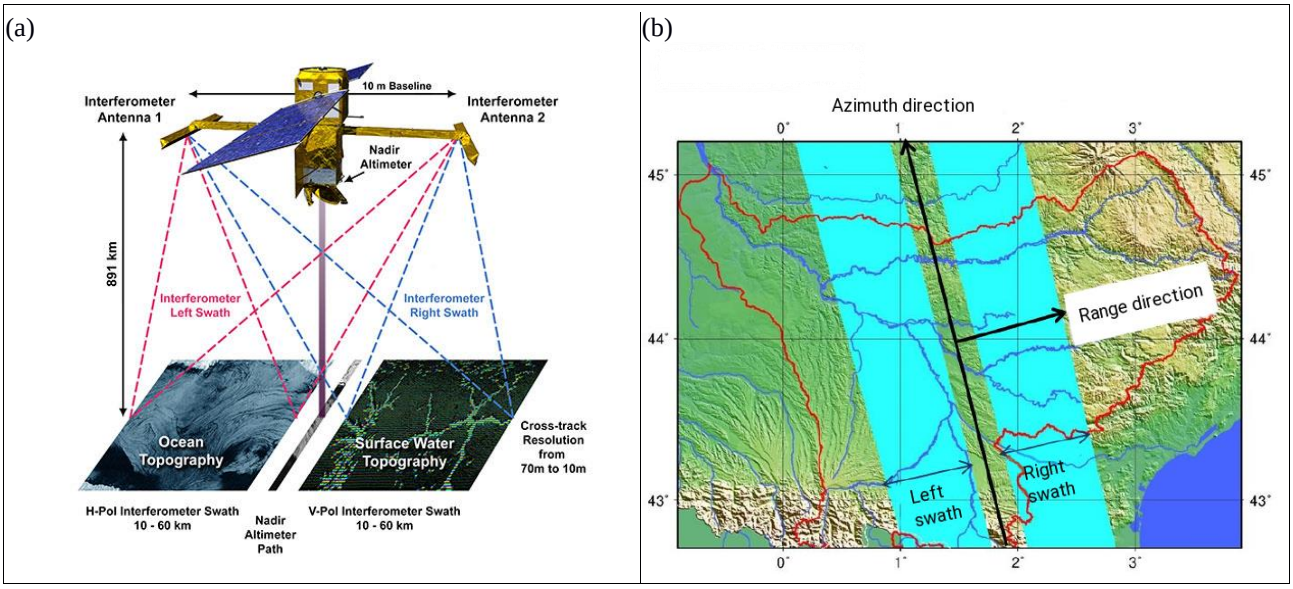

Figure 2: (a) Illustration of SWOT (© NASA - http://swot.jpl.nasa.gov/): the widths of the two rectangles represent two swaths of 50 km wide, observed by the two antennas of the satellite. They can observe either ocean or continental open water surfaces. (b) Illustration of the left and right swaths of SWOT, with the range direction perpendicular to the satellite track (which is the azimuth direction)

Preprints (www.preprints.org) | NOT PEER-REVIEWED | Posted: 27 October 2018 doi:10.20944/preprints201810.0643.v1

Peer-reviewed version available at Water 2019, 11, 78; doi:10.3390/w11010078

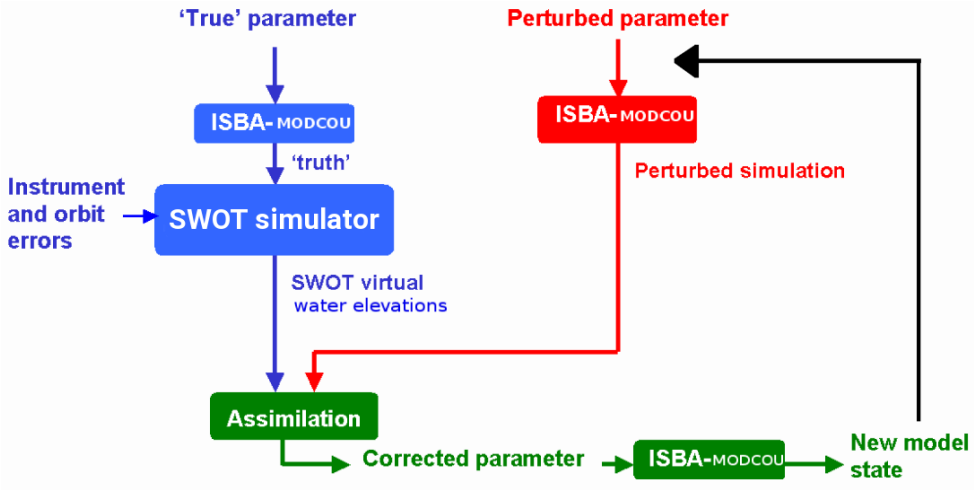

Figure 3: Schematic illustration of twin experiment. The red boxes describe the perturbed parameters of the model (SIM_PERT). The blue boxes represent the truth SIM_TRUE (reference simulation) by adding a white noise corresponding to the SWOT measurement error. The green boxes represent the corrected parameters of the model after a DA window: we obtain corrected parameters of the model (SIM_ANA) being used for the next DA window (black line), allowing the calculation of new corrected parameters at the next window's termination.

Preprints (www.preprints.org) | NOT PEER-REVIEWED | Posted: 27 October 2018 doi:10.20944/preprints201810.0643.v1

Peer-reviewed version available at Water 2019, 11, 78; doi:10.3390/w11010078

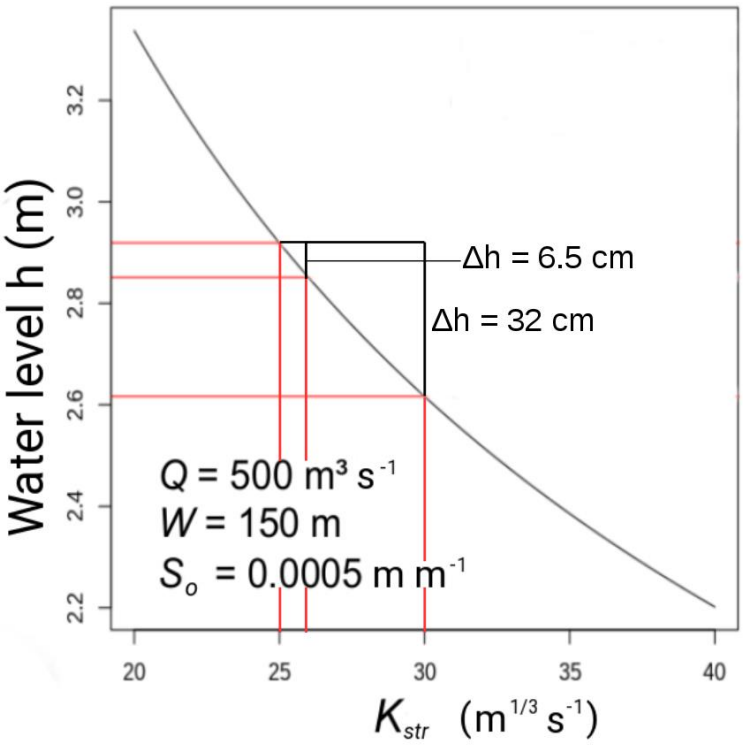

Figure 4: River depth *h* as a function of the roughness coefficient K_{str}, for a large rectangular river channel, with geomorphological parameters and a discharge value typical of large plain rivers

Preprints (www.preprints.org) | NOT PEER-REVIEWED | Posted: 27 October 2018 doi:10.20944/preprints201810.0643.v1

Peer-reviewed version available at Water 2019, 11, 78; doi:10.3390/w11010078

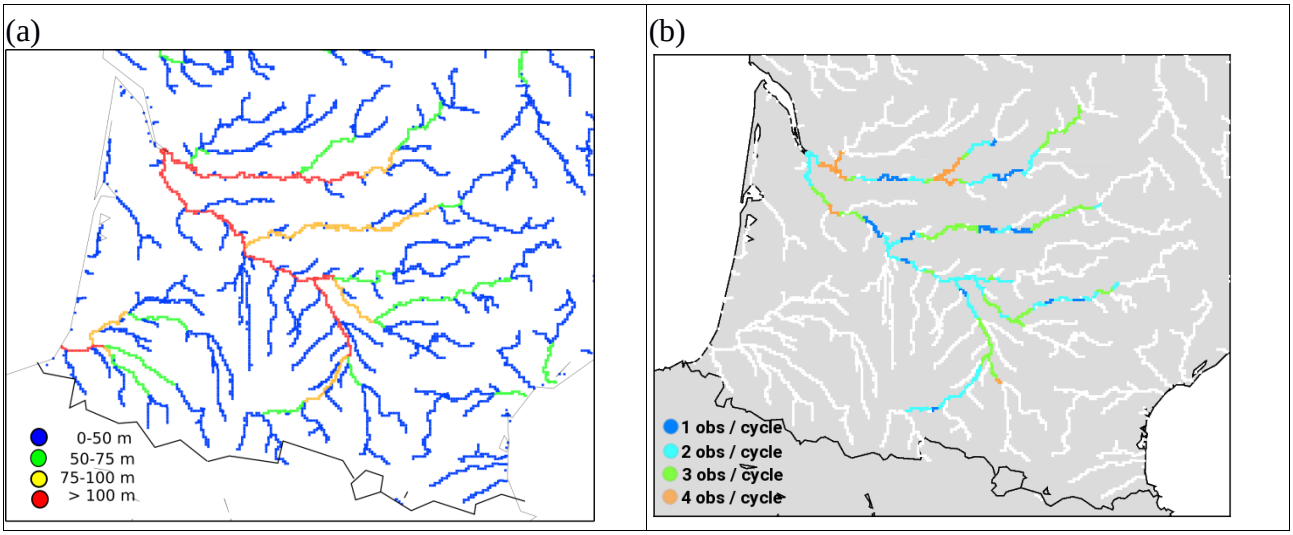

Figure 5: (a) River widths computed in the DA platform over the Garonne catchment, considering three river width classes where virtual SWOT observations are assimilated; (b) SWOT observation number for a 21-day cycle for every 10-km reaches of the Garonne catchment

Preprints (www.preprints.org) | NOT PEER-REVIEWED | Posted: 27 October 2018 doi:10.20944/preprints201810.0643.v1

Peer-reviewed version available at Water 2019, 11, 78; doi:10.3390/w11010078

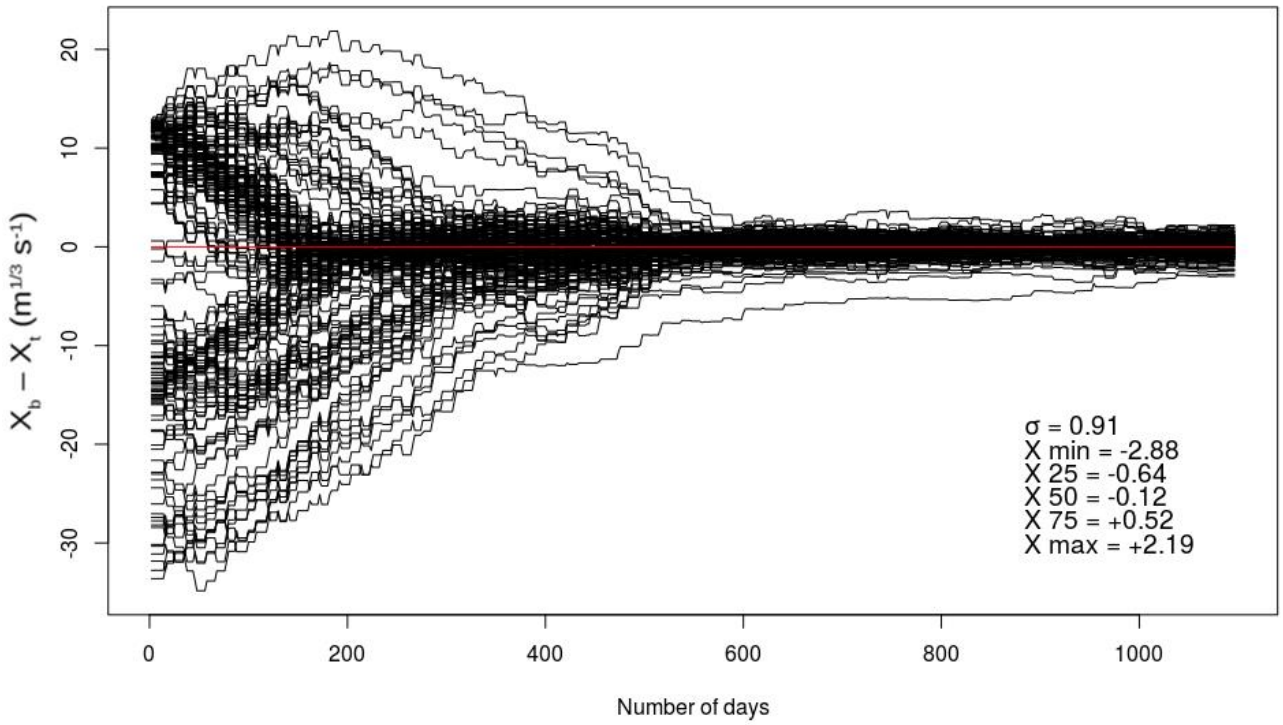

Figure 6: Temporal evolution (01/08/1995 to 31/07/1998) of the difference between the a priori control vector (x_b) and the true control vector (x_t) of the Strickler coefficients in the DA system. The 165 black curves represent the value (x_b-x_t) at all 165 reaches defined over the Garonne catchment. The red horizontal line is equivalent to a zero difference between x_b and x_t. After 3 years (i.e. 548 48h-assimilation windows), we represent the standard deviation σ_{xb} between the 165 values (x_b–x_t) in the basin. The X terms represent from top to bottom the minimum value, the 1st quartile, the 2nd quartile, the mediane, the 3rd quartile and the maximum value of (x_b–x_t) at the end of the experiment (day n° 1096).

Preprints (www.preprints.org) | NOT PEER-REVIEWED | Posted: 27 October 2018 doi:10.20944/preprints201810.0643.v1

Peer-reviewed version available at Water 2019, 11, 78; doi:10.3390/w11010078

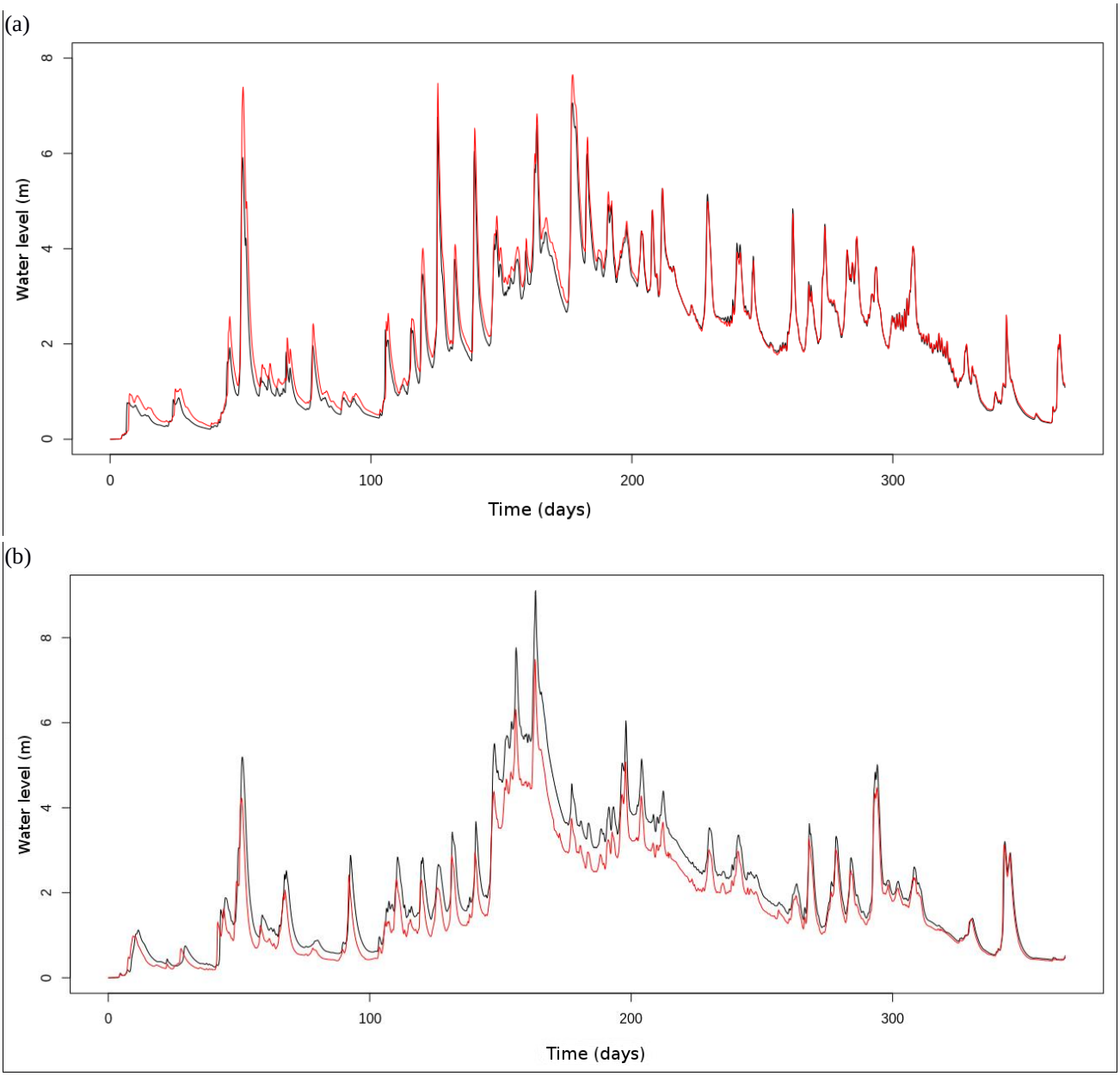

Figure 7: Temporal evolution of the river depth at Lamagistère (a) and Bergerac (b), over the period 01/08/1995 to 31/071996. Black curves correspond to the truth and red curves to the analyzed river depth

Preprints (www.preprints.org) | NOT PEER-REVIEWED | Posted: 27 October 2018 doi:10.20944/preprints201810.0643.v1

Peer-reviewed version available at Water 2019, 11, 78; doi:10.3390/w11010078

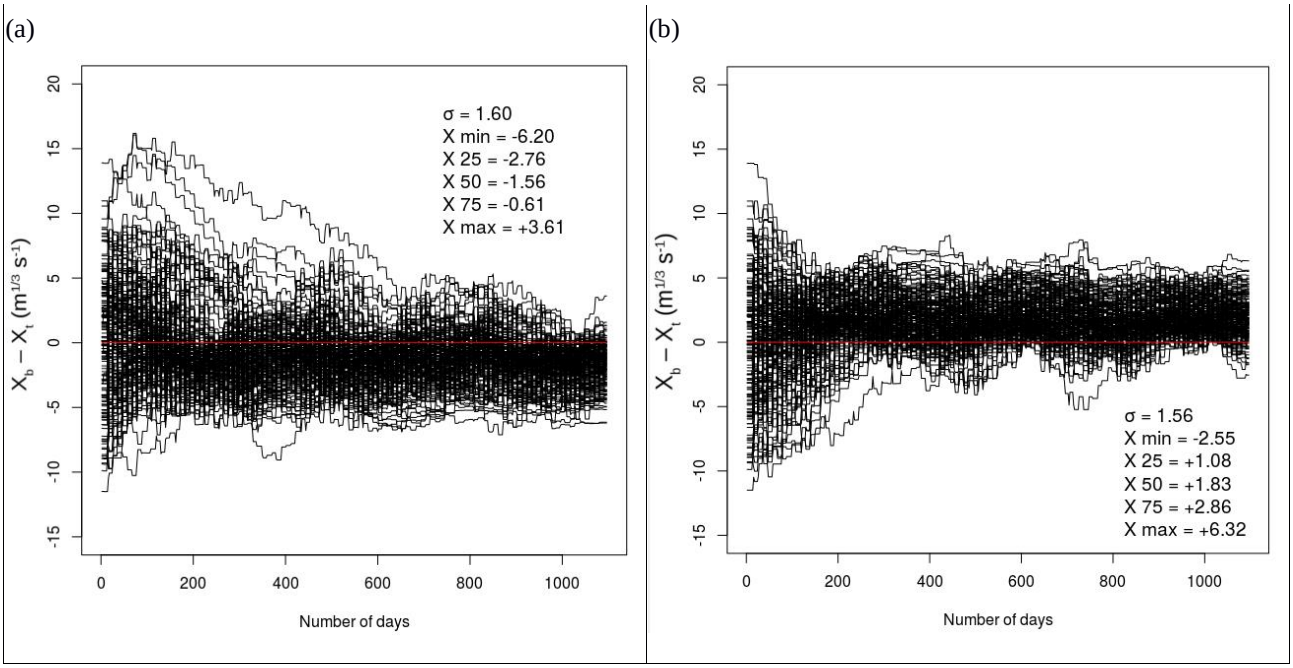

Figure 8: Temporal evolution (01/08/1995 to 31/07/1998) of the difference between the a priori control vector (x_b) and the true control vector (x_t) of the Strickler coefficients in the DA system. The scenario (a) represents a -10 % perturbation of water produced by ISBA, and the scenario (b) represents a +10 % perturbation. The 165 black curves represent the value (x_b-x_t) af all 165 reaches defined over the Garonne catchment. The red horizontal line is equivalent to a zero difference between x_b and x_t. After 3 years (i.e. 548 48h-assimilation windows), we represent the standard deviation σ_{xb} between the 165 values (x_b–x_t) in the basin. The X terms represent from top to bottom the minimum value, the 1st quartile, the 2nd quartile, the mediane, the 3rd quartile and the maximum value of (x_b–x_t) at the end of the experiment (day n° 1096).

Preprints (www.preprints.org) | NOT PEER-REVIEWED | Posted: 27 October 2018 doi:10.20944/preprints201810.0643.v1

Peer-reviewed version available at Water 2019, 11, 78; doi:10.3390/w11010078

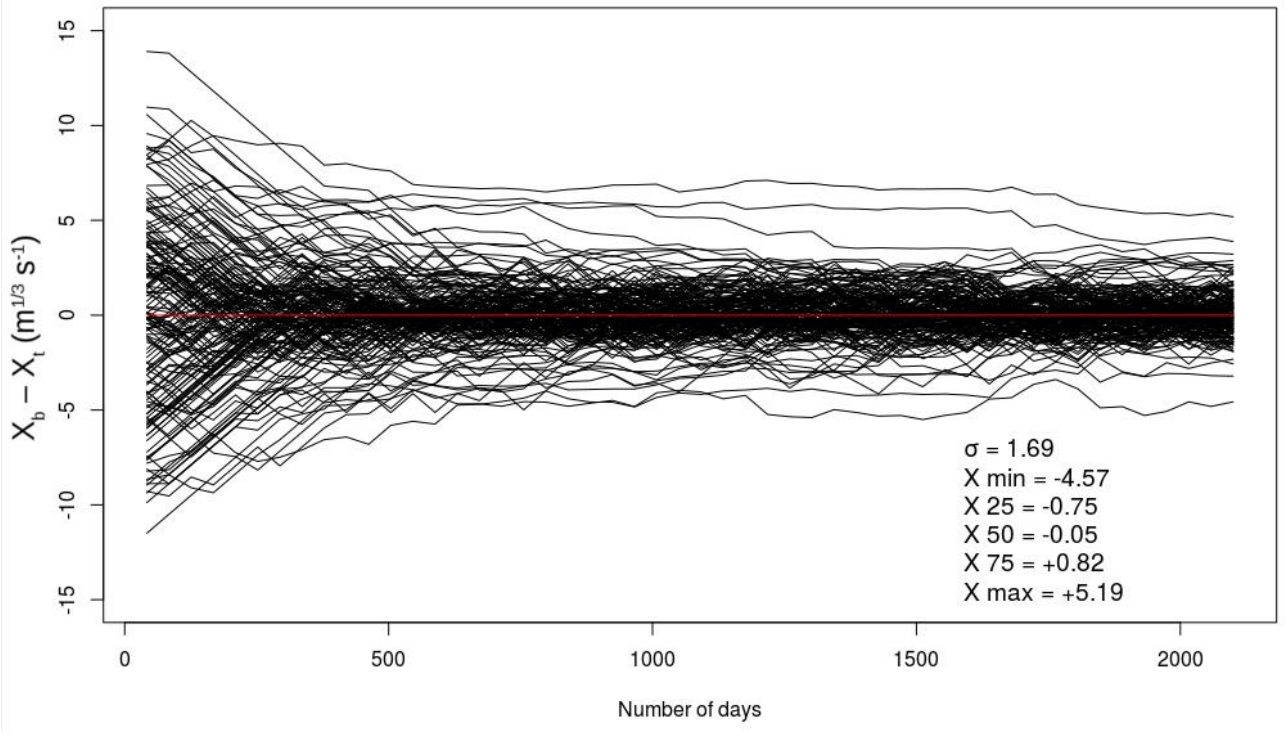

Figure 9: Temporal evolution (01/08/1995 to 15/04/2001) of the difference between the a priori control vector (x_b) and the true control vector (x_t) of the Strickler coefficients in the DA system. The 165 black curves represent the value (x_b-x_t) at all 165 reaches defined over the Garonne catchment. The red horizontal line is equivalent to a zero difference between x_b and x_t. After 5 years (i.e. 50 42 day-assimilation windows), we represent the standard deviation σ_{xb} between the 165 values (x_b–x_t) in the basin. The X terms represent from top to bottom the minimum value, the 1st quartile, the 2nd quartile, the mediane, the 3rd quartile and the maximum value of (x_b-x_t) at the end of the experiment (day n° 2100).

Preprints (www.preprints.org) | NOT PEER-REVIEWED | Posted: 27 October 2018 doi:10.20944/preprints201810.0643.v1

Peer-reviewed version available at *Water* **2019**, *11*, 78; doi:10.3390/w11010078

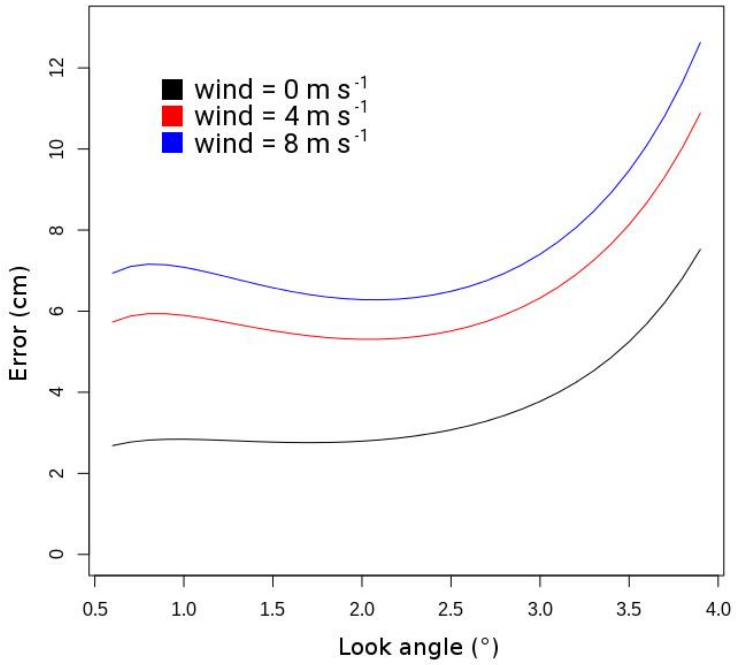

Figure 10: SWOT error measurement as a function of the look angle for a wind speed of 0 m s^{-1}, 4 m s^{-1} or 8 m s^{-1}

Preprints (www.preprints.org) | NOT PEER-REVIEWED | Posted: 27 October 2018 doi:10.20944/preprints201810.0643.v1

Peer-reviewed version available at Water 2019, 11, 78; doi:10.3390/w11010078

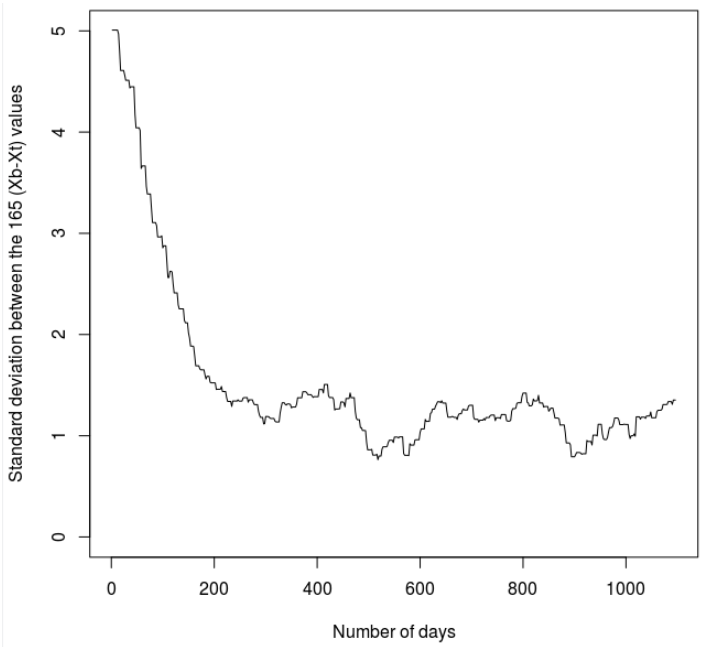

Figure 11: Temporal evolution of the standard deviation σ between the 165 (x_b–x_t) terms, over the 01/08/1995 - 31/07/1998 period

Preprints (www.preprints.org) | NOT PEER-REVIEWED | Posted: 27 October 2018 doi:10.20944/preprints201810.0643.v1

Peer-reviewed version available at *Water* **2019**, *11*, 78; doi:10.3390/w11010078

Δ K_{str}	**Averaged Δ*h***
-5 % (-1.5 $m^{1/3}$ s^{-1}) +5 % (+1.5 $m^{1/3}$ s^{-1})	+1.5 cm +1.0 cm
-20 % (-6 $m^{1/3}$ s^{-1})	+7.5 cm
+20 % (+6 $m^{1/3}$ s^{-1})	+3.5 cm

Table 1: Impact of the relative and absolute perturbation of the K_{str} reference coefficient on the river depths *h* (cm)

Preprints (www.preprints.org) | NOT PEER-REVIEWED | Posted: 27 October 2018 doi:10.20944/preprints201810.0643.v1

Peer-reviewed version available at Water 2019, 11, 78; doi:10.3390/w11010078

Symbol	Variable	Dimension
x_b	A priori vector of the Strickler coefficients	165
x_t	Truth vector of the Strickler coefficients	165
x_a	Analysis vector of the Strickler coefficients	165
y_o	Observation vector of the synthetic SWOT river depths during a DA window	p
$H(x_b)$	Model equivalent of the y_o vector, with the river depths simulated by RAPID during a DA window	p
R	Observation error matrix of river depths	p x p
B	Model error matrix of Strickler coefficients	165 x 165
H	Jacobian matrix : sensitivity of $H(x_b)$ to a perturbation of the Strickler coefficient in the model	165 x p

Table 2: Synthetic description of the variables used in the assimilation equations (symbol, description and dimension). The p value corresponds to the number of SWOT observations during a DA window.

Preprints (www.preprints.org) | NOT PEER-REVIEWED | Posted: 27 October 2018 doi:10.20944/preprints201810.0643.v1

Peer-reviewed version available at Water 2019, 11, 78; doi:10.3390/w11010078

Criterion	**EXPERIMENT 1: river depth assimilation**	**EXPERIMENT 2: river depth assimilation by perturbing ISBA outputs**	**EXPERIMENT 3: Difference of river depth assimilation**	**EXPERIMENT 4: river depth assimilation considering more realistic SWOT errors**
Assimilation type	River depths	River depths ; ISBA runoff and drainage perturbed ±10 %	river depth differences	River depths
Window duration	48 hours	48 hours	42 days	48 hours
Beginning of the experiment	01/08/1995	01/08/1995	01/08/1995	01/08/1995
End of the experiment	31/07/1998	31/07/1998	15/04/2001	31/07/1998
First *a priori* value x_b	Each value of Strickler coefficient are equal to 25 $m^{1/3}$ s^{-1}	«Truth» of the 165 Strickler coefficient values perturbed with a centered gaussian noise σ_{xb} equal to 5 $m^{1/3}$ s^{-1}	«Truth» of the 165 Strickler coefficient values perturbed with a centered gaussian noise σ_{xb} equal to 5 $m^{1/3}$ s^{-1}	«Truth» of the 165 Strickler coefficient values perturbed with a centered gaussian noise σ_{xb} equal to 5 $m^{1/3}$ s^{-1}
Definition of the matrix **B**	Diagonal, each value σ_B^2 is equal to the variance of all the x_b values around the truth. Minimum imposed value = (1.5 $m^{1/3}$ s^{-1})²	Diagonal, each value σ_B^2 is equal to the variance of all the x_b values around the truth. Minimum imposed value = (1.5 $m^{1/3}$ s^{-1})²	Diagonal, each value σ_B^2 is equal to the variance of all the x_b values around the truth. Minimum imposed value = (2.12 $m^{1/3}$ s^{-1})²	Diagonal, each value σ_B^2 is equal to the variance of all the x_b values around the truth. Minimum imposed value = (1.5 $m^{1/3}$ s^{-1})²
Definition of the matrix **R**	Diagonal, each value σ_R^2 is equal to (10 cm)²	Diagonal, each value σ_R^2 is equal to (10 cm)²	Diagonal, each value σ_R^2 is equal to (10 cm)²	Diagonal, each value σ_R^2 varies in the time and the space

Table 3: Synthetic description of the four SWOT DA experiments

Preprints (www.preprints.org) | NOT PEER-REVIEWED | Posted: 27 October 2018 doi:10.20944/preprints201810.0643.v1

Peer-reviewed version available at Water 2019, 11, 78; doi:10.3390/w11010078

Hydrology error component	Height error (cm)
Ionosphere signal (constant)	0.80
Dry troposphere signal (constant)	0.70
Wet troposphere signal (variable)	4.00
Orbit radial component (constant)	1.62
KaRIn Random and systematic errors after cross-over correction (constant)	7.74
Surface of the reach + look angle + wind speed (variable)	4.40
Total allocation	9.95
Unallocated margin (constant)	1.04
Total error	10.0

Table 4: SWOT error measurement allocation (Brown and Obligis 2014), after averaging over a 1 km² area (Rodríguez 2016). The left column represents the error component, and the right columns represents the values of these errors.